Micellar Structure of Hydrophobically Modified Polysaccharides in Aqueous Solution

Takahiro Sato,[1,*] Jia Yang,[1,2] and Ken Terao[1]

[1] Department of Macromolecular Science, Osaka University, 1-1 Machikaneyama-cho, Toyonaka, Osaka 560-0043, Japan

[2] College of Science, Shenyang University of Chemical Technology, 11th Street, Shenyang Economic and Technological Development Zone, Shenyang 110142, China

[1]Tel: +81-6-6850-5462, Fax: +81-6-6850-5461, E-mail: tsato@chem.sci.osaka-u.ac.jp

Running Head: Hydrophobically Modified Polysaccharides in Solution

Abstract

This article reviews previous studies on the micellar structure formed by hydrophobically modified polysaccharides in aqueous solutions, by static and dynamic light scattering, small angle X-ray and neutron scattering, and fluorescence from pyrene solubilized in the polymer solution. Those experimental results are consistently explained by the full or loose flower necklace model for pullulan bearing octenyl groups and amylose bearing dodecyl groups, and by the randomly branched polymer model, which is often called as “nanogel,” for pullulan bearing cholesteryl groups. We discuss the micellar structures of those hydrophobically modified polysaccharides as well as of an amphiphilic alternating vinyl polymer bearing dodecyl groups, depending on the degree of substitution as well as chemical structures of the hydrophobic moiety and backbone chain.

Key Words: hydrophobically modified polysaccharides / pullulan / amylose / micelle / flower necklace / scattering / fluorescence

Introduction

Polysaccharides derivatives have attracted much attention in the field of drug delivery systems, because of their biocompatibility, biodegradability, and non-toxicity.[1-5] In 1993, Akiyoshi et al.[6] synthesized cholesterol-bearing pullulan (CHP) and found self-aggregation to form nano-particles (nanogels) and complexation with globular proteins, proposing the applications as nano-carriers for lipophilic drugs and proteins. Afterwards, they reported that the nanogels of CHP can refold heat-denatured enzymes.[7,8] In 1994, Ohya et al.[9] synthesized glutaraldehyde-crosslinked chitosan nano-particle bearing an anti-cancer drug. This work was followed by vast reports of chitosan-based nano-particles[1-3] including poly(ethylene glycol)-grafted chitosan,[10] ionically crosslinked chitosan particles,[11] and polyelectrolyte complexes of chitosan and polyanion.[12] More recently, Eenschooten et al.[13] synthesized amphiphilic hyaluronic acid derivative reacted with octenyl succinic anhydride (OSA), and proposed to use as the drug delivery system.

Amphiphilic random copolymers with vinyl polymer backbones are known to form flower micelles or flower necklaces in aqueous media.[14-18] Although hydrophobically modified polysaccharides, like above CHP and OSA-modified hyaluronic acid, are amphiphilic random copolymers, their micellar structures in aqueous solutions have been little investigated in detail. Only recently, Kameyama et al.[19] and Yang and Sato[20-22] investigated micellar structures of an amphiphilic amylose derivate (C12CMA) and hydrophobically modified pullulan, respectively. Especially, the latter authors synthesized OSA-modified pullulan (PUL-OSA; cf. Fig. 1) according to the method of Eenschooten, Tømmeraas, et al.,[13,23-25] and thoroughly studied dependences of its micellar structure in 0.05 M aqueous NaCl on the degree of polymerization ($N_{0,1}$) and on the degree of substitution (*DS*) by small-angle X-ray scattering (SAXS),

fluorescence from solubilized pyrene prove, and size-exclusion chromatography equipped with online multi-angle light scattering detector (SEC-MALS).

In this focus review, we briefly explain micellar structural studies of CHP, C12CMA, and PUL-OSA on the basis of the flower necklace model. The backbone of hydrophobically modified polysaccharides consists of saccharide residues, which is considerably different from the vinyl polymer backbone, consisting of ethylene units. It is intrigued to compare the micellar structure of PUL-OSA with those of amphiphilic vinyl copolymers[16,17] in aqueous media on the basis of the flower necklace model.

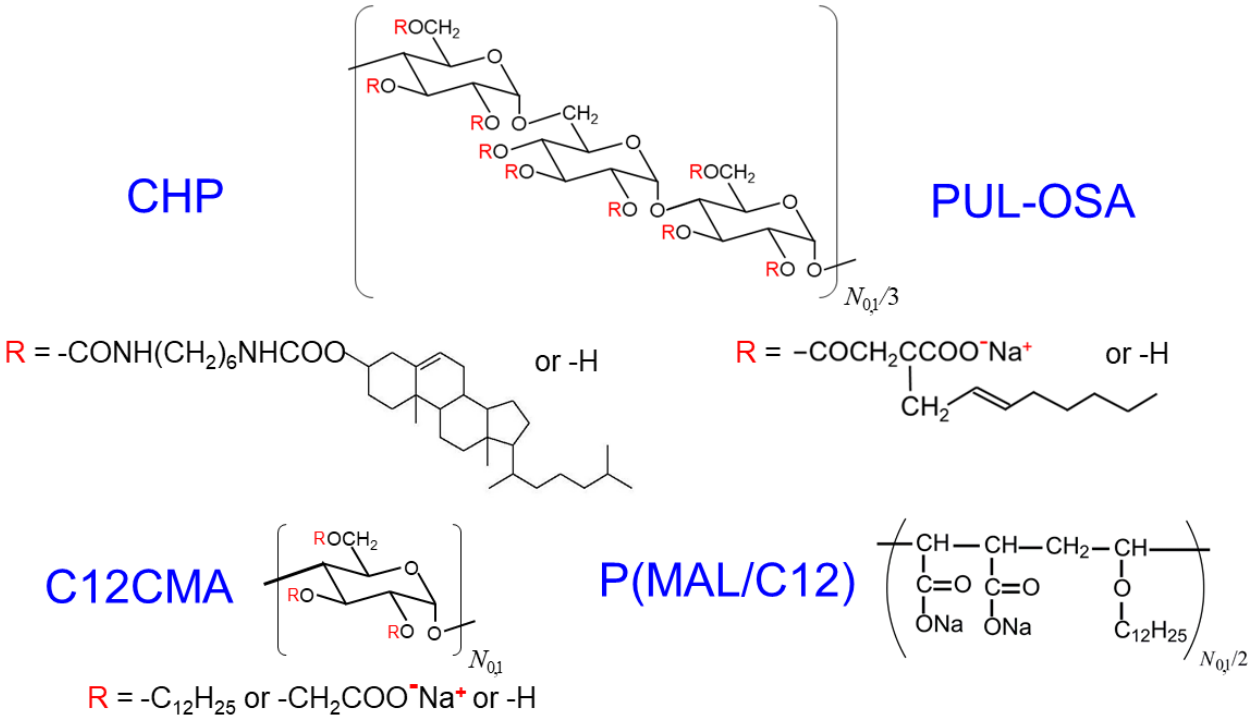

Fig. 1 Chemical structures of amphiphilic random and alternating copolymers reviewed in this article.

In what follows, the PUL-OSA sample code, like P20DS90, indicates the molecular weight (or molar mass in units of kg/mol) of PUL before substitution by the number after P, and *DS* (in

mol%) by the number after DS, while CHP samples are coded as CHP-*X*-*Y* where *X* is the molecular weight (in units of kg/mol) of PUL before substitution and *Y* is *DS* (in mol%). C12CMA samples are named as C12CMA*Y*-*Z* where *Y* and *Z* are *DS* (in mol%) of dodecyl and carboxymethyl groups, respectively.

Micelle models

Let us consider amphiphilic random and alternating copolymers. The single copolymer backbone chain without forming the micelle is regarded as a wormlike chain[26] with the persistence length q and the contour length L. When the single copolymer chain comprises $N_{0,1}$ monomer units of which contour length is h, the total contour length L is equal to $hN_{0,1}$. The monomer unit is the glucose residue for pullulan and amylose derivatives and the ethylene unit for P(MAL/C12), and $N_{0,1}$ is referred to as the degree of polymerization in what follows. The copolymer chain bears hydrophobic groups (the cholesteryl, octenyl, and dodecyl groups) with the degree of substitution *DS* (i.e., the number of hydrophobic group(s) per monomer unit). In an aqueous solution, the amphiphilic copolymers form a micelle. The number of copolymer chains per micelle (the aggregation number) is denoted as m, and the number of monomer units per micelle N_0 is equal to $mN_{0,1}$.

Fig. 2 illustrates micelle models proposed for amphiphilic random and alternating copolymers.[14-18,21] The flower micelle consists of loop chains and hydrophobic core formed by hydrophobic groups. It is noted that the contour length shorter than $l_{\mathrm{loop}} \equiv 1.6q$ cannot take the loop conformation because of its chain stiffness.[26,27] Thus, if *DS* is higher than h/l_{loop}, the loop size must be fixed to the minimum loop size l_{loop}, and not all hydrophobic groups of the copolymer chain can enter the hydrophobic core (cf. Figure S1 in the Supporting Information).

The flower micelle is characterized in terms of l_{loop} and the number of minimum-size loops n_{loop}. If the contour length L of the copolymer chain exceeds $l_{loop}n_{loop}$, or $N_0 = mN_{0,1}$ exceeds $N_{0,u} \equiv l_{loop}n_{loop}/h$, the copolymer chain(s) may take the flower necklace conformation with n_c hydrophobic cores (cf. Figure S2 in the Supporting Information). The transition from the flower micelle to the flower necklace by changing $N_{0,1}$ was observed for P(MAL/C12)[16] in dilute aqueous solution. (If the bridge chain is energetically unfavorable, each copolymer chain cannot form two or more bridge chains in the multi-core micelle, and the branched architecture may be prohibited.)

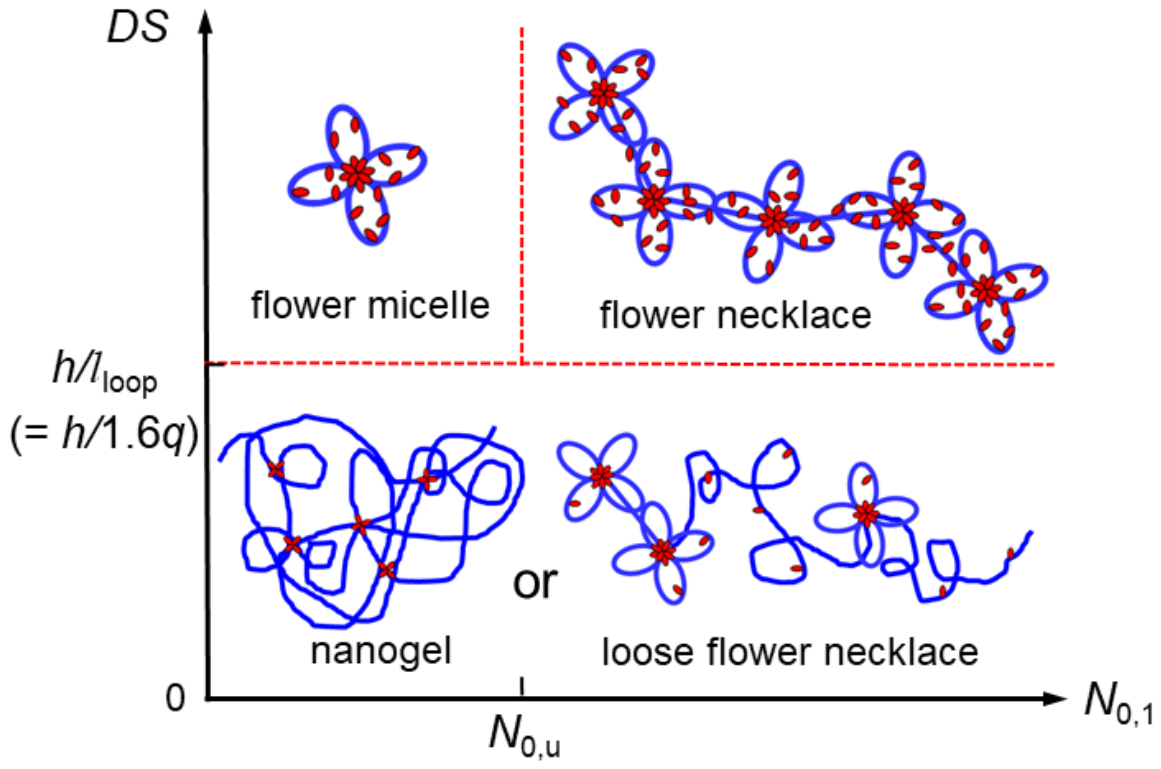

Fig. 2 Schematic illustration of micelle models proposed for amphiphilic random and alternating copolymers.

When DS is lower than h/l_{loop}, the loop size is not fixed to be l_{loop}, but can be larger than l_{loop} (cf. Figure S1 in the Supporting Information). The micelle formed by random copolymers with such low DS may be viewed as a randomly branched polymer with subchains of a random distribution,[28] and is referred to as the "nanogel", according to Akiyoshi et al.[8] If the distribution of hydrophobic groups along the backbone chain is not random but multi-block copolymer-like, some unit flower micelles may remain on subchains with locally high hydrophobic group densities, even if the average DS is lower than h/l_{loop}. The loose flower necklace consists of n_c unit flower micelles and n_l random coil subchains.[21] In what follows, the contour length of the random coil subchain is assumed to be also $N_{0,u}$ for simplicity.

Fluorescence from pyrene solubilized in aqueous micellar solutions

A hydrophobic fluorophore, pyrene, is often used to study the hydrophobic micro-domain in aqueous micellar solutions. For example, Fig. 3a and b show fluorescence spectra and decay curves of pyrene solubilized in aqueous micellar solutions of a PUL-OSA sample P20DS90 at the copolymer mass concentration $c = 0.9 \times 10^{-3}$ g/cm^3 and three different pyrene molar concentrations [Py]. Below 420 nm, the spectra do not depend on the pyrene concentration solubilized, and the ratio I_3/I_1 of the third (383 nm) to first (372 nm) peak intensities is 0.92, which is definitely larger than the ratio for pyrene in water (= 0.63),[29] and comparable to those in aqueous micellar solutions of sodium dodecyl sulfate (SDS) (= 0.96).[30] On the other hand, above 420 nm of the wavelength, an additional broad peak appears around 475 nm with increasing the pyrene concentration. This peak corresponds to the fluorescence emission from the pyrene excimer formed in the solution of higher pyrene concentrations.[31] The formation of the pyrene

excimer makes fluorescence around 400 nm decay more rapidly in a short time region, as demonstrated in Panel b. From the fraction of the rapidly decaying component, we can estimate the average number $\overline{n}$ of pyrene molecules existing in a micellar hydrophobic core.

Fig. 3c collects I_3/I_1 data in solutions of PUL-OSA with different *DS* and $N_{0,1}$, as well as of C12CMA and P(MAL/C12) bearing dodecyl hydrophobes and of CHP with very hydrophobic cholesteryl moieties. The ratios are above 0.9 for PUL-OSA with octenyl groups at $DS > 0.5$, and for C12CMA and P(MAL/C12) bearing dodecyl hydrophobes even at $DS \leq 0.5$. The I_3/I_1 value in the CHP solution is as high as 0.8 at a few % *DS*. Those I_3/I_1 values indicate that solubilized pyrene molecules are mostly included in hydrophobic micro-domains, demonstrating the micelle formation of these amphiphilic copolymers in the aqueous solutions.

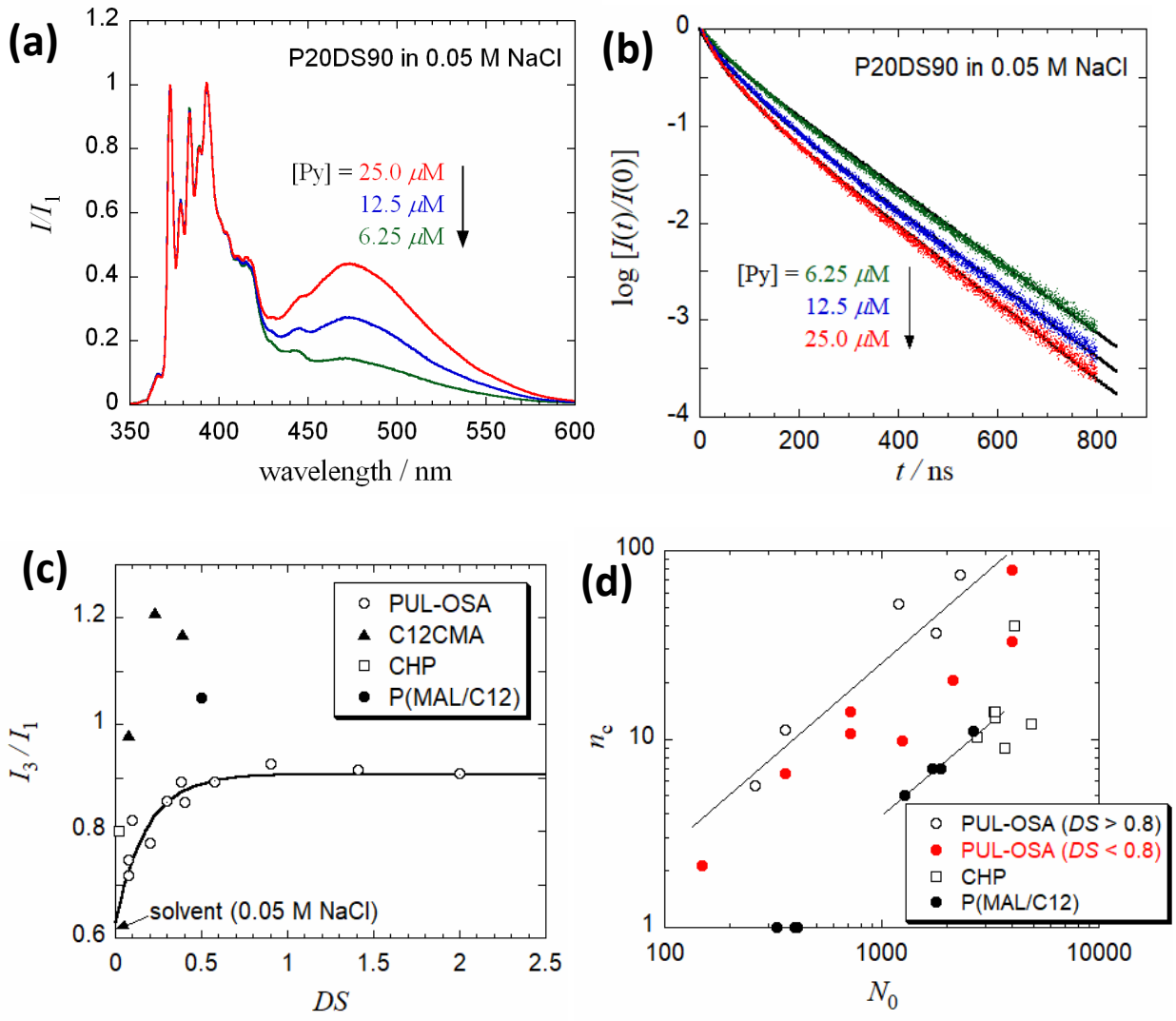

Fig. 3 Fluorescence spectra (a) and decay curves (b) for pyrene solubilized in 0.05 M aqueous NaCl solutions of a PUL-OSA sample (P20DS90 with $N_{0,1}$ = 142 and *DS* = 0.90) at the copolymer mass concentration $c = 0.9 \times 10^{-3}$ g/cm^3 and three different pyrene concentrations,[20] (c) ratios I_3/I_1 of pyrene solubilized in aqueous solutions of PUL-OSA,[20,21] C12CMA,[19] CHP,[32] and P(MAL/C12)[16] (the solid curve, eye guide), and (d) numbers n_c of hydrophobic cores per micelle obtained from fluorescence decay curves for aqueous solutions of PUL-OSA,[20,21] and P(MAL/C12),[16] as well as from the steady-state fluorescence quenching experiment for aqueous

solutions of CHP.[32] Reproduced with permission from ref 20. Copyright (2020) American Chemical Society.

As mentioned below, scattering experiments provide us the number of monomer units N_0 per micelle, and we can estimate the number of hydrophobic cores n_c from [Py](M_0N_0/N_A)/($c\,\overline{n}$), where M_0 is the molar mass of the monomer unit using $\overline{n}$ estimated by the fluorescence decay curve (cf. Fig. 3b). Circles in Fig. 3d indicate the results of n_c calculated by this method for PUL-OSA and P(MAL/C12). Data points for PUL-OSA with $DS > 0.8$ and P(MAL/C12) with $N_0 >$ 1000 almost obey straight lines with the slope of unity, expected for the flower necklace model (cf. Fig. 2). The molar concentration of the hydrophobic core (= [Py]/$\overline{n}$) can be obtained by the steady-state fluorescence quenching experiment.[33] Square symbols in Fig. 3d show the results of n_c for CHP using this experiment.[32] The proportionality between n_c and N_0 does not hold for CHP, so that multi-core micelle formed by CHP in water is not the flower necklace (see below).

Scattering from aqueous micellar solutions

More detailed information about the micellar structure can be provided by various scattering experiments, small-angle X-ray scattering (SAXS), small-angle neutron scattering (SANS), static light scattering (SLS), and dynamic light scattering (DLS). The key parameter in the scattering experiments is the magnitude of the scattering vector (or the scattering wavenumber) k, calculated by $(4\pi/\lambda)\sin(\theta/2)$ with the wavelength λ of the radiation in the solution and the scattering angle θ. Due to the difference in λ, SLS and DLS usually cover k ranging roughly from 0.005 nm^{-1} to 0.03 nm^{-1}, while SAXS and SANS roughly from 0.05 nm^{-1} to 2 nm^{-1}. Thus,

SLS and DLS give us the information of global structure of the micelle, and SAXS and SANS provide the information of more local structure.

Fig. 4a compares SAXS profiles for PUL-OSA samples with different *DS* (and $N_{0,1}$) in 0.05 M aqueous NaCl. Here, $R_{\theta,X}$ is the excess Rayleigh ratio of SAXS, K_e is the SAXS optical constant, and *c* is the polymer mass concentration. The profile for a pullulan homopolymer, P100, has a plateau in a low *k* region, and monotonically decreases with increasing *k*, which can be fitted by the wormlike chain perturbed by the excluded volume effect (cf. the dot-dash curve in the figure).[34,35] On the other hand, the profiles for PUL-OSA with $DS \geq 0.38$ show a minimum at $k \sim 1.5$ nm^{-1}. Such SAXS profiles are expected for flower micelles with the hydrophobic core of low electron density. Because the electron density of hydrocarbons is generally low, the (unit) flower micelle with the hydrophobic core constructed by hydrocarbons can be viewed as such a double-layered sphere. Thus, the PUL-OSA micelles with $DS \geq 0.38$ possess the unit flower micellar structure. (The profile for the sample P100DS20 does not possess a minimum, but exhibits a slightly negative curvature around $k = 1$ nm^{-1}, which can be regarded as a symptom of the unit flower micellar structure.) In Fig. 4b, the SAXS profiles of the two C12CMA samples, C12CMA39-90 and C12CMA23-90, have a similar minimum at $k \approx 1$ nm^{-1}, indicating that the two C12CMA samples also form a micelle with the (unit) flower micellar structure.

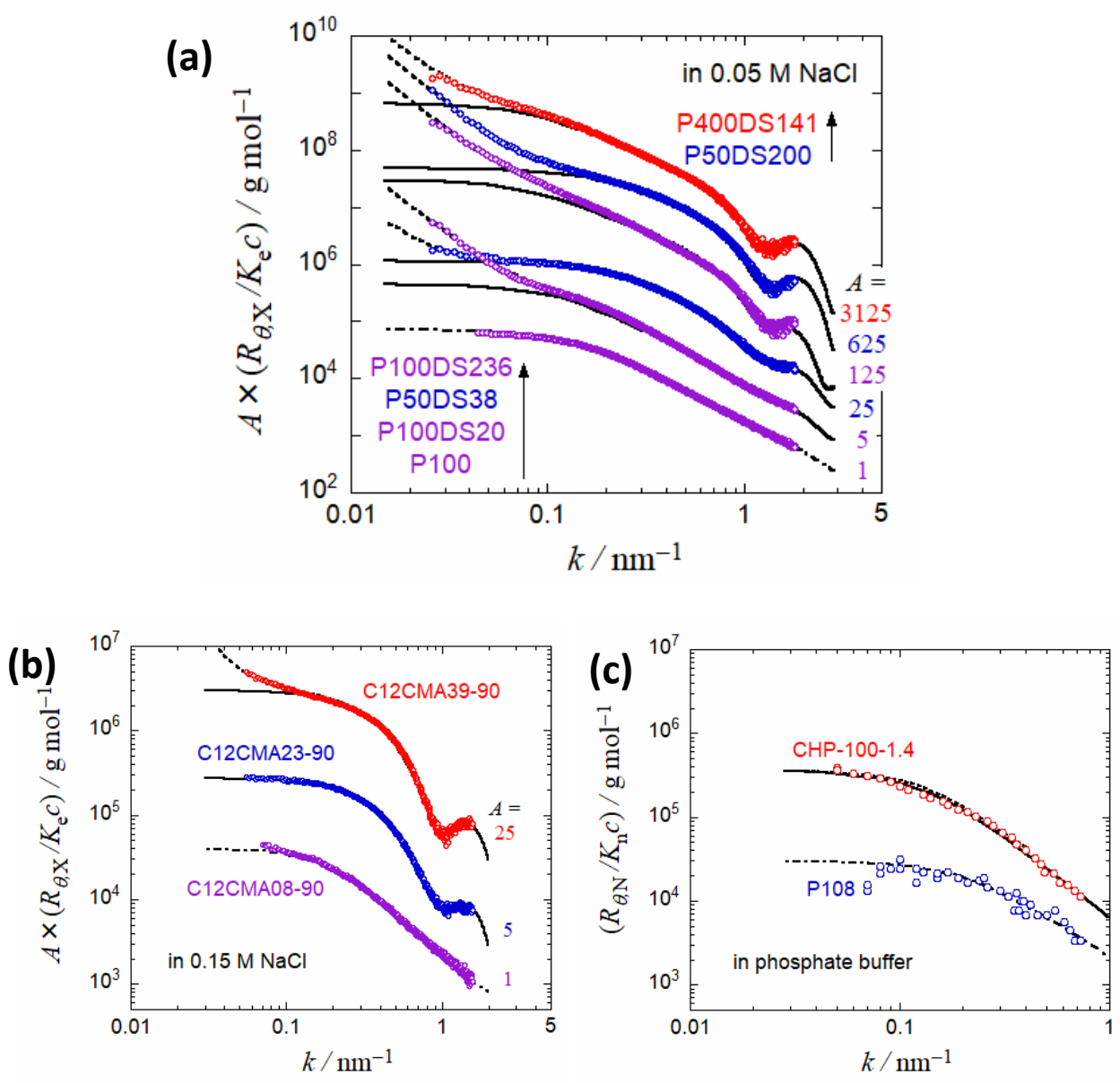

Fig. 4 SAXS profiles for PUL-OSA samples in 0.05 M aqueous NaCl at 25 °C (c = 0.26–1.2 × 10^{-2} g/cm^3)[20,21] (a) and for C12CMA samples in 0.15 M aqueous NaCl at 25 °C (infinite dilution),[19] as well as SANS profiles for CHP and the mother pullulan sample P100 in phosphate buffer at 25 °C (c = 1.0 × 10^{-2} g/cm^3).[36] Profiles in Panels a and b other than P100 and C12CMA08-90 are shifted vertically by the factor A indicated in the panel. Solid and dashed

curves indicate fitting results explained in the text; dot-dash curves are the fitting results by the wormlike chain perturbed by the excluded volume effect.[34,35]

Yang and Sato[20,21] fitted SAXS profiles for micelles formed by 13 PUL-OSA samples with different *DS* and $N_{0,1}$ by the flower necklace or loose flower necklace model (cf. Fig. 2). Solid curves in Fig. 4a indicate the fitting results, where n_c values chosen were consistent with the results obtained by the fluorescence experiments (cf. Fig. 3d). Except in low k regions, the experimental SAXS profiles are nicely fitted by the theoretical curves. The same fitting was made on the SAXS profiles for C12CMA39-90 and C12CMA23-90 (cf. solid curves in Fig. 4b) by using the flower necklace model with $n_c \approx 3$. Agreements between experiment and theory are slightly better than the previous fitting,[19] where the concentric double cylinder model was used. We will discuss the fitting parameters in the next subsection.

The profiles for PUL-OSA, as well as for C12CMA39-90, exhibit an upswing in a lower k region. This indicates that the PUL-OSA and C12CMA micelles partly form higher aggregates in the aqueous solutions. Because the scattering power of the higher aggregates is very strong, a tiny amount of the higher aggregates can induce the enhanced scattering intensity at low scattering angles. In fact, the addition of the fractal-aggregate scattering component can fit the experimental SAXS profiles by assuming a negligibly small amount of the aggregating component (cf. dashed curves in Fig. 4a).[20,21] We do not discuss here the details of the higher aggregates of micelles.

In Fig. 4c, the SANS profile for the sample CHP-100-1.4 is compared with that for the mother pullulan sample P100.[36] Here, $R_{\theta,N}$ and K_n are the excess Rayleigh ratio of SANS and the SANS optical constant, respectively. The low angle plateau value for CHP-100-1.4 is higher than

that for P100, indicating that CHP-100-1.4 forms self-aggregates in buffer solution, but the profile itself resembles that for the random coil chain. In fact, the profile can be fitted by the Debye function for the linear Gaussian chain with the weight average molar mass $M_w = 4.7 \times 10^5$ g/mol,[37] and the radius of gyration $\langle S^2 \rangle^{1/2} = 12$ nm, as indicated by the solid curve in Fig. 4c. (The apparent second virial coefficient A_2 was chosen to be 3×10^{-5}cm^{3}g^{-2}mol.)

As mentioned in the previous subsection, the steady-state fluorescence quenching experiment indicated that CHP chains form "nanogels" possessing multiple hydrophobic cores making up of a few cholesteryl groups attached to CHP.[32] If the hydrophobic cores are regarded as branch points, the CHP nanogel may be viewed as a randomly branched polymer. The scattering function for the randomly branched polymer can be calculated by the theory of Kurata and Fukatsu[28] (cf. Supporting Information). As demonstrated by dotted curve in Fig. 4c, the scattering function for the randomly branched polymer is not so much different from that for the linear chain (the solid curve), when the functionality f is chosen to be 4, and the number of branch points m is calculated from $DS(M_w/M_0)/(f/2) = 19$ along with $M_w = 4.7 \times 10^5$ g/mol, $\langle S^2 \rangle^{1/2} = 11$ nm, $A_2 = 3 \times 10^{-5}$ cm^{3}g^{-2}mol, and the molar mass per the glucose residue $M_0 = 170$ g/mol. Due to the ill convergence of the power series expansion given by eq S6, it was difficult to calculate the scattering function at $k > 0.4$ nm^{-1}, and we cannot distinguish between the nanogel and linear chain by the SANS profile. It is noted that unless the sample is not deuterium labeled, the difference in the SANS contrast factor between hydrophilic and hydrophobic core domains within the micelle is not so large, that SANS profile does not exhibit the characteristic minimum unlike the SAXS profile. (In the original paper,[36] the SANS profile for CHP-100-1.4 was fitted to the uniform-density sphere model, which provided a slightly stronger k dependence in the high k region than experiment.)

The aggregation number m of copolymer chains per micelle as well as the radius of gyration $\langle S^2 \rangle^{1/2}$ of the micelle can be determined from SAXS and SANS profiles in low k region after eliminated the contribution of the higher aggregating component of the micelle. The same parameters may be obtained also by SLS after eliminated the contribution of the higher aggregating component using DLS data.[16,38] As shown in Fig. 5a, values of m for PUL-OSA[20,21] over all $N_{0,1}$ investigated as well as for P(MAL/C12)[16] at $N_{0,1} > 1000$ are less than 2, indicating that those micelles are close to the "unimer micelle." On the other hand, m for P(MAL/C12)[16] at $N_{0,1} < 300$ and for CHP[32] show approximately the inverse proportionality to $N_{0,1}$. As mentioned above, P(MAL/C12) at $N_{0,1} < 300$ form the uni-core flower micelle with $n_c = 1$. As demonstrated theoretically, the uni-core flower micelle is constructed by a constant optimum number of monomer units $N_{0,u}$. This optimum number is given by $mN_{0,1}$, so that $m = N_{0,u}/N_{0,1}$. On the other hand, CHP forms multi-core micelle, and there is no reason for the inverse proportionality to $N_{0,1}$. CHP nanogels have been dispersed so far by sonication after the CHP sample was mixed with the solvent.[32] The sonication may disperse the nanogels to an optimum size.

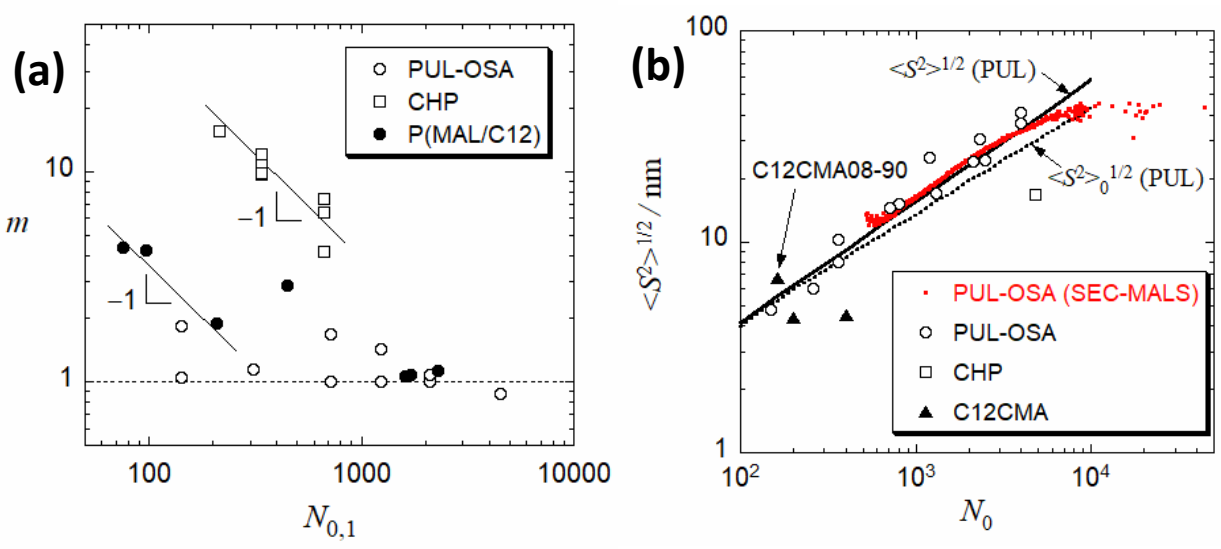

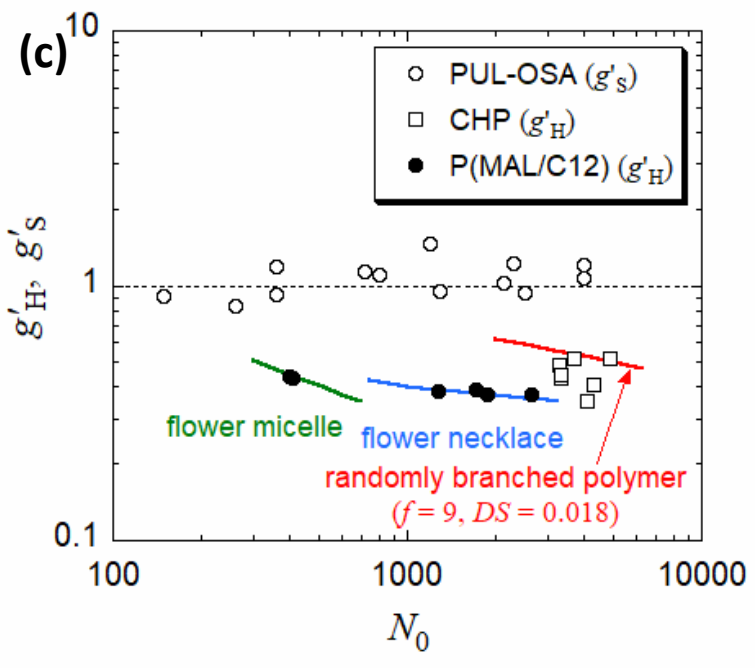

Fig. 5 (a) Aggregation number m of copolymer chains per micelle,[16,20,21,32] (b) the radius of gyration $\langle S^2 \rangle^{1/2}$,[6,19-22] and (c) the shrinking factors g'_H and g'_S for micelles of amphiphilic random and alternating copolymers.[17,20,21,32]

Fig. 5b shows N_0 dependences of $\langle S^2 \rangle^{1/2}$ for the micelles of PUL-OSA, CHP, and C12CMA. Comparing with $\langle S^2 \rangle^{1/2}$ for pullulan (PUL) without hydrophobes (the solid curve),[34] we can say that the dimension of PUL-OSA does not essentially change, but that of CHP shrinks by the micellization. (The dotted curve in Fig. 5b is the radius of gyration of PUL in the unperturbed state.) Although $\langle S^2 \rangle^{1/2}$ for C12CMA without bearing hydrophobes (i.e., C12CMA0-90) has not reported, it should be close to that for C12CMA08-90, and C12CMA shrinks by the micellization in a contrast with PUL-OSA. Red small circles in Fig. 5b indicate the SEC-MALS (the size-exclusion chromatograph equipped with an online multi-angle light scattering detector) results for micelles of a PUL-OSA sample with DS = 0.2, synthesized from a polydisperse PUL

sample.[22] While data points at $N_0 < 4000$ almost obey the solid curve for PUL, being consistent with the SAXS results,[20] those at $N_0 < 4000$ deviate downward from the curve, which may correspond to the higher aggregates of the PUL-OSA micelle detected also by SAXS.[20]

Just like the g factor for branched polymers, we define the shrinking factors g'_S for the radius of gyration and g'_H for the hydrodynamic radius due to the micellization by the ratio of the radius of gyration (or the hydrodynamic radius) for the micelle to that for the linear chain with the same N_0 as the micelle and $DS = 0$ in the same solvent condition. (It is noted that the g factor for the radius of gyration for branched polymers is conventionally defined as the ratio with respect to the mean *square* radius of gyration, which is different from our definition of g'_S.) From the results in Fig. 5b, we can calculate g'_S for PUL-OSA, and similarly calculate g'_H for CHP[32] and P(MAL/C12).[17] The results are shown in Fig. 5c. As already mentioned, g'_S for PUL-OSA is approximately unity. On the other hand, g'_H for CHP and P(MAL/C12) are considerably less than unity. The hydrodynamic radii for the flower micelle and the flower necklace of P(MAL/C12) were calculated previously.[16,17] Using the previous results, we obtain the green and blue curves for P(MAL/C12), which agree with the experimental data points at 400 and at $N_0 > 1000$, respectively. If the nanogel of CHP is regarded as the randomly branched polymer mentioned above, g_H is calculated by the theory of Kurata and Fukatsu[28] (cf eq S8 in Supporting Information). The red curve in Fig. 5c is their theoretical result for CHP with $DS = 0.018$ (the averaged value of the CHP samples used in ref 32) with $f = 9$ (the half of the average number of cholesteryl groups per hydrophobic core estimated by the steady-state fluorescence quenching experiment.[32]).

Parameters characterizing the micelles

As mentioned above, three amphiphilic random and alternating copolymers, PUL-OSA, C12CMA, and P(MAL/C12) form the flower necklace in aqueous solution. The structure of the flower necklace can be characterized in terms of the contour length of the loop chain (l_{loop}), the number of loops or petals per unit flower micelle (n_{loop}), the average radius of the hydrophobic core ($\overline{R}_{core}$), the number of unit flower micelles (n_c) shown in Fig. 3d, and the persistence length of the flower necklace ($q_{necklace}$). Now, we compare these structural parameters of flower necklaces formed by the three different copolymers.

First of all, the contour length of the loop chain l_{loop} is 2.9 nm for PUL-OSA, 3.2 nm for C12CMA, and 4.8 nm for P(MAL/C12). The electrostatic contribution of the persistence length q for the copolymer backbone chain may affect the values of l_{loop} (= $1.6q$) especially for P(MAL/C12) with the high charge density. Fig. 6a compares n_{loop} and $\overline{R}_{core}$ obtained by the fits of SAXS profiles for the three copolymers (cf. Fig. 4a and b). The number of petals n_{loop} per unit flower micelle for PUL-OSA is smaller than those for P(MAL/C12) and C12CMA. This may be owing to the shorter chain length of the octenyl group attached to PUL-OSA than that of the dodecyl group of P(MAL/C12) and C12CMA, which reduces the aggregation number of hydrophobes per hydrophobic core, and then n_{loop}. From the same reason, most of average radii of the hydrophobic core $\overline{R}_{core}$ determined by SAXS for PUL-OSA are slightly smaller than those for C12CMA (Fig. 6a). However, $\overline{R}_{core}$ for P(MAL/C12) is comparable with those for PUL-OSA. When the SAXS profiles for PUL-OSA and C12CMA in Fig. 4a and b are compared with SAXS profiles for P(MAL/C12) (cf. Figure 1 in ref. 17), the latter profiles possess a much sharper minimum, implying that the hydrophobic core structure of P(MAL/C12) is considerably different from that of hydrophobically modified polysaccharides. We have to investigate in more

detail the structure of the hydrophobic core formed by amphiphilic copolymers. The persistence length q_{necklace} of the flower necklace is (6 ± 2) nm for PUL-OSA, 3.5 nm for C12CMA, and 7 nm for P(MAL/C12), all of which are larger than the persistence length q of the copolymer backbone chain.

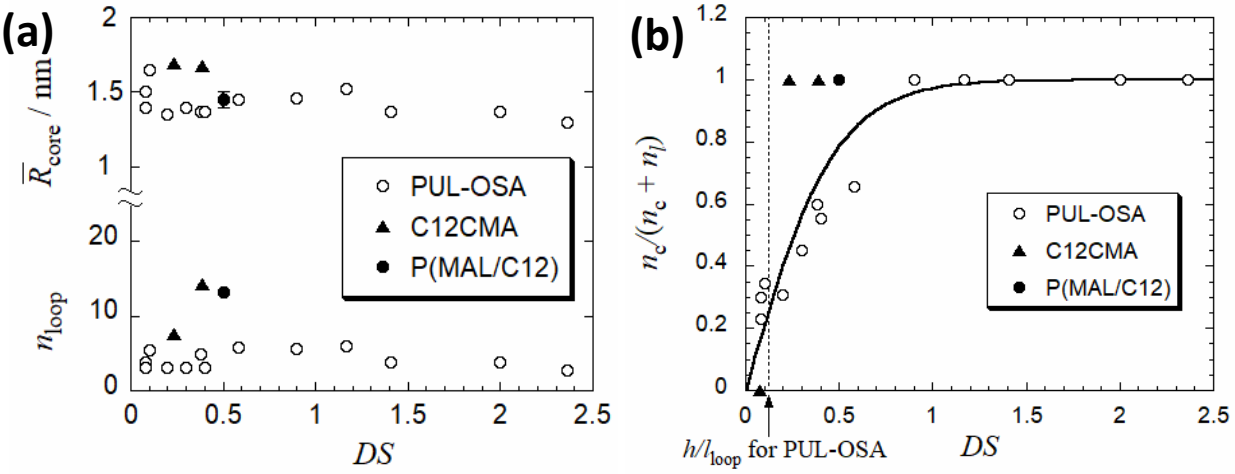

Fig. 6 *DS* dependences of n_{loop} and $\overline{R}_{\text{core}}$ (a), as well as $n_c/(n_c + n_l)$ (b) for PUL-OSA,[20,21] C12CMA,[19] and P(MAL/C12)[17] micelles.

As already mentioned above, data points of n_c for PUL-OSA with $DS < 0.8$, shown by gray circles in Fig. 3d deviate downward from the line followed by data points for PUL-OSA with $DS > 0.8$, and moreover the SAXS profile for the sample P100DS20 in Fig. 4a exhibits a slightly negative curvature around $k = 1$ nm^{-1}, indicating that the unit flower micelle partly remains even at *DS* 0.2. These results imply that PUL-OSA with low *DS* takes the loose flower necklace conformation. In fact, the solid curves for P50DS38 and P100DS20 in Fig. 4a were calculated using the loose flower necklace model with n_c unit flower micelles and n_l random coil subchains. Fig. 6b shows the fraction $n_c/(n_c + n_l)$ of the unit flower micelle in the loose flower necklace,

used for the fits of the SAXS profiles. The fraction decreases from unity at $DS < 0.8$ for PUL-OSA. This is in a contrast with the fact that C12CMA exists in aqueous solution as the full flower necklace even at *DS* as low as 0.23.

As mentioned in the second subsection, the copolymer chain does not necessarily form the minimum-size loops, when *DS* is lower than h/l_{loop}. In Fig. 6b, the vertical dotted line indicates *DS* being equal to h/l_{loop} (= 0.12) for PUL-OSA, which is considerably lower than *DS* where $n_c/(n_c + n_l)$ for PUL-OSA starts deviating from unity. Therefore, the unit flower micelle may not be formed even if two or more hydrophobic octenyl groups are borne on the copolymer chain portion with the contour length of l_{loop} on average. However, we should notice the method for synthesizing PUL-OSA, which was prepared by the substitution reaction with OSA oil droplets in aqueous solution. The substitution reaction may occur at train portions of the PUL chain adsorbed on OSA droplet surface, but not at loop and tail portions of the PUL chain.[39,40] This reaction mechanism may introduce the heterogeneity in the distribution of octenyl groups along the PUL backbone chain especially at low DS, which affects the DS dependence of the micellar structure.

Conclusions

Hydrophobically modified pullulan bearing octenyl or cholesteryl groups (PUL-OSA and CHP) and amylose bearing dodecyl groups (C12CMA) as hydrophobic moieties assemble micelles in aqueous solutions, where hydrophobic moieties attached to polysaccharide chains aggregate to form hydrophobic cores. PUL-OSA bearing octenyl groups with relatively weak hydrophobicity can form stable micelles over a wide range of the degree of substitution *DS*, while CHP with cholesteryl groups of stronger hydrophobicity is dispersible in water only in a low *DS* range.

Micellar structures of PUL-OSA, CHP, and C12CMA in aqueous media were studied by SLS, DLS, SAXS, SANS, and fluorescence from pyrene solubilized in the copolymer solution. All the experimental results were consistently explained by the full or loose flower necklace model for PUL-OSA and C12CMA, and by the randomly branched polymer model for CHP. The latter model may be identified with the "nanogel" model proposed by Akiyoshi et al.[32,37]

The micellar structure is affected by *DS* and $N_{0,1}$ (the degree of polymerization; cf. Fig 2) as well as chemical structures of the hydrophobic moiety and backbone chain. With decreasing *DS*, the micelle of PUL-OSA transforms from full to loose flower necklace. While the global dimension (the hydrodynamic radius) of the flower necklace for C12CMA and P(MAL/C12) (the amphiphilic alternating copolymer of sodium maleate and dodecyl vinyl ether) is smaller than that of the random coil for the linear chain with the same N_0 (the number of repeating units per micelle), the radius of gyration of the PUL-OSA flower necklace is even slightly larger than that of the random-coiled PUL chain before the hydrophobic modification. Although the contour length of the flower necklace for PUL-OSA shrinks from the contour length of the PUL chain by the formation of unit flowers, the flower necklace is considerably stiffer than the PUL chain, and the stiffness compensates the contour length shrinkage. This resembles the global dimension of polymacromonomers.[41,42] As a common feature, both PUL-OSA and P(MAL/C12) form unimer micelle with $m = 1$ at high degrees of polymerization.

ASSOCIATED CONTENT

Supporting Information

The Supporting Information on dependences of the micellar structure on the degree of substitution and degree of polymerization, as well as particle scattering function and shrinking factors for the randomly branched polymer is available.

AUTHOR INFORMATION

Corresponding Author

*(T.S.) E-mail tsato@chem.sci.osaka-u.ac.jp.

ORCID

Takahiro Sato: 0000-0002-8213-7531

Notes

The authors declare no competing financial interest.

ACKNOWLEDGEMENT

We thank Dr. Daichi Ida at Kyoto University for correcting eq 24 of ref 28, and Dr. Shin-ichi Yusa at the University of Hyogo and Dr. Akihito Hashidzume at Osaka University for valuable discussion. This work was supported in part by JSPS KAKENHI Grant No. 18H02020. The synchrotron radiation experiments were performed at the BL40B2 of SPring-8 with the approval of the Japan Synchrotron Radiation Research Institute (JASRI) (Proposal No. 2019B1375, 2016B1088, 2015B1100, 2015A1179, 2014B1715, and 2014B1087).

References

1. Janes KA, Calvo P, Alonso MJ. Polysaccharide colloidal particles as delivery systems for

macromolecules. Adv Drug Deliv Rev. 2001; 47: 83–97.

2. Prabaharan M, Mano JF. Chitosan-based particles as controlled drug delivery systems. Drug Deliv. 2005; 12: 41-57.
3. Liu Z, Jiao Y, Wang Y, Zhou C, Zhang Z. Polysaccharides-based nanoparticles as drug delivery systems. Adv Drug Deliv Rev. 2008; 60: 1650-1662.
4. Prajapati VD, Jani GK, Khanda SM. Pullulan: an exopolysaccharide and its various applications. Carbohydr Polym. 2013; 95: 540-549.
5. Singh RS, Kaur N, Rana V, Kennedy JF. Pullulan: a novel molecule for biomedical applications. Carbohydr Polym. 2017; 171: 102-121.
6. Akiyoshi K, Deguchi S, Moriguchi N, Yamaguchi S, Sunamoto J. Self-aggregates of hydrophobized polysaccharides in water. formation and characteristics of nanoparticles. Macromolecules. 1993; 26: 3062-3068.
7. Akiyoshi K, Sasaki Y, Sunamoto J. Molecular chaperone-like activity of hydrogel nanoparticles of hydrophobized pullulan: thermal stabilization with refolding of carbonic anhydrase B. Bioconjugate Chem. 1999; 10: 321-324.
8. Nomura Y, Sasaki Y, Takagi M, Narita T, Aoyama Y, Akiyoshi K., Thermoresponsive controlled association of protein with a dynamic nanogel of hydrophobized polysaccharide and cyclodextrin: heat shock protein-like activity of artificial molecular chaperone. Biomacromolecules. 2005; 6: 447-452.
9. Ohya Y, Shiratani M, Kobayashi H, Ouchi T. Release behavior of 5-fluorouracil from chitosan-gel nanospheres immobilizing 5-fluorouracil coated with polysaccharides and their cell specific cytotoxicity. Pure Appl Chem. 1994; A31: 629–642.

10. Ouchi T, Nishizawa H, Ohya Y. Aggregation phenomenon of PEG-grafted chitosan in aqueous solution. Polymer. 1998; 39: 5171-5175.
11. Calvo PC, Remuñán-López C, Vila-Jato JL, Alonso MJ. Novel hydrophilic chitosan–polyethylene oxide nanoparticles as protein carriers. J Appl Polym Sci. 1997; 63: 125–132.
12. Mumper RJ, Wang J, Claspell JM, Rolland AP. Novel polymeric condensing carriers for gene delivery. Proc Intl Symp Control Rel Bioact Mater. 1995; 22: 178–179.
13. Eenschooten C, Guillaumie F, Kontogeorgis GM, Stenby EH, Schwach-Abdellaoui K. Preparation and structural characterisation of novel and versatile amphiphilic octenyl succinic anhydride–modified hyaluronic acid derivatives. Carbohydr Polym. 2010; 79: 597-605.
14. Kawata T, Hashidzume A, Sato T. Micellar structure of amphiphilic statistical copolymers bearing dodecyl hydrophobes in aqueous media. Macromolecules. 2007**;** 40: 1174-1180.
15. Tominaga Y, Mizuse M, Hashidzume A, Morishima Y, Sato T. Flower micelle of amphiphilic random copolymers in aqueous media. J. Phys. Chem. B. 2010; 114: 11403-11408.
16. Ueda M, Hashidzume A, Sato T. Unicore−multicore transition of the micelle formed by an amphiphilic alternating copolymer in aqueous media by changing molecular weight. Macromolecules. 2011; 44: 2970-2977.
17. Uramoto K, Takahashi R, Terao K, Sato T. Local and global conformations of flower micelles and flower necklaces formed by an amphiphilic alternating copolymer in aqueous solution. Polym J. 2016; 48: 863–867.
18. Sato T. Theory of the flower micelle formation of amphiphilic random and periodic copolymers in solution. Polymers. 2018; 10: 73.

19. Kameyama Y, Kitamura S, Sato T, Terao K. Self-assembly of amphiphilic amylose derivatives in aqueous media. Langmuir. 2019; 35: 6719-6726.
20. Yang J, Sato T. Micellar structure of a hydrophobically modified pullulan in an aqueous solution. Macromolecules. 2020; 53: 7970−7979.
21. Yang J, Sato T. Transition from the random coil to the flower necklace of a hydrophobically modified pullulan in aqueous solution by changing the degree of substitution. Polymer. 2021; 214: 123346.
22. Yang J, Sato T. Characterization of the Micelle Formed by a Hydrophobically Modified Pullulan in Aqueous Solution: Size Exclusion Chromatography. Polymers. 2021; 13: 1237.
23. Eenschooten C, Vaccaro A, Delie F, Guillaumie F, Tømmeraas K, Kontogeorgis GM, Schwach-Abdellaoui K, Borkovec M, Gurny R. Novel self-associative and multiphasic nanostructured soft carriers based on amphiphilic hyaluronic acid derivatives. Carbohydr Polym. 2012**;** 87: 444-451.
24. Neves-Petersen MT, Klitgaard S, Skovsen E, Petersen SB, Tømmeraas K, Schwach-Abdellaoui K. Biophysical properties of phenyl succinic acid derivatised hyaluronic acid. J Fluoresc. 2010; 20: 483–492.
25. Tømmeraas K, Mellergaard M, Malle BM, Skagerlind P. New amphiphilic hyaluronan derivatives based on modification with alkenyl and aryl succinic anhydrides. Carbohydr Polym. 2011; 85: 173-179.
26. Yamakawa H, Yoshizaki T. Helical wormlike chains in polymer solutions, 2nd ed.; Springer: Berlin/Heidelberg, Germany, 2016; ISBN 978-3-662–48714–3.
27. Yamakawa H, Stockmayer WH. Statistical mechanics of wormlike chains. II. Excluded volume effects. J Chem Phys. 1972; 57: 2843–2854.

28. Kurata M, Fukatsu M. Unperturbed dimension and translational friction constant of branched polymers. J Chem Phys. 1964; 41: 2934-2944.
29. Kalyanasundaram K, Thomas JK. Environmental effects on vibronic band intensities in pyrene monomer fluorescence and their application in studies of micellar systems. J Am Chem Soc. 1977; 99: 2039–2044.
30. Lianos P, Zana R. Use of pyrene excimer formation to study the effect of NaCl on the structure of sodium dodecyl sulfate micelles. J Phys Chem. 1980; 84: 3339-3341.
31. Hashidzume A, Kawaguchi A, Tagawa A, Hyoda K, Sato T. Synthesis and structural analysis of self-associating amphiphilic statistical copolymers in aqueous media. Macromolecules. 2006; 39: 1135–1143.
32. Akiyoshi K, Deguchi S, Tajima H, Nishikawa T, Sunamoto J. Microscopic structure and thermoresponsiveness of a hydrogel nanoparticle by self-assembly of a hydrophobized polysaccharide. Macromolecules. 1997; 30: 857-861.
33. Turro NJ, Yekta A. Luminescent probes for detergent solutions. A simple procedure for determination of the mean aggregation Nnmber of micelles. J Am Chem Soc. 1978; 100: 5951-5952.
34. Yang J, Sato T. Conformation of pullulan in aqueous solution studied by small-angle X-ray scattering. Polymers. 2020; 12: 1266.
35. Pedersen JS, Schurtenberger P. Scattering Functions of Semiflexible Polymers with and without Excluded Volume Effects. Macromolecules. 1996; 29: 7602–7612.
36. Inomoto N, Osaka N, Suzuki T, Hasegawa U, Ozawa Y, Endo H, Akiyoshi K, Shibayama M. Interaction of nanogel with cyclodextrin or protein: Study by dynamic light scattering and small-angle neutron scattering. Polymer. 2009; 50: 541-546.

37. Kuroda K, Fujimoto K, Sunamoto J, Akiyoshi K. Hierarchical self-assembly of hydrophobically modified pullulan in water: gelation by networks of nanoparticles. Langmuir. 2002; 18: 3780-3786.

38. Kanao M, Matsuda Y, Sato T. Characterization of Polymer Solutions Containing a Small Amount of Aggregates by Static and Dynamic Light Scattering. Macromolecules. 2003; 36: 2093-2102.

39. C. Eenschooten, Development of soft nanocarriers from novel amphiphilic, Ph.D. Thesis, in Hyaluronic Acid Derivatives towards Drug Delivery, Technical University of Denmark, 2008.

40. Kawaguchi Y, Matsukawa K, Ishigami Y. Conformational changes of hyaluronates with partial palmitoylation and the adsorption structures on the surface of oil droplets. Carbohydr Polym. 1993; 20: 183-187.

41. Terao K, Farmer BS, Nakamura Y, Iatrou H, Hong K, Mays JM. Radius of Gyration of Polystyrene Combs and Centipedes in a Θ Solvent. Macromolecules. 2005; 38: 1447-1450.

42. Zhang B, Gro1hn F, Pedersen JS, Fischer K, Schmidt M. Conformation of Cylindrical Brushes in Solution: Effect of Side Chain Length. Macromolecules. 2006; 39: 8440-8450.

Figure legends:

Fig. 1 Chemical structures of amphiphilic random and alternating copolymers reviewed in this article.

Fig. 2 Schematic illustration of micelle models proposed for amphiphilic random and alternating copolymers.

Fig. 3 Fluorescence spectra (a) and decay curves (b) for pyrene solubilized in 0.05 M aqueous NaCl solutions of a PUL-OSA sample (P20DS90 with $N_{0,1}$ = 142 and DS = 0.90) at the copolymer mass concentration $c = 0.9 \times 10^{-3}$ g/cm^3 and three different pyrene concentrations,[20] (c) ratios I_3/I_1 of pyrene solubilized in aqueous solutions of PUL-OSA,[20,21] C12CMA,[19] CHP,[32] and P(MAL/C12)[16] (the solid curve, eye guide), and (d) numbers n_c of hydrophobic cores per micelle obtained from fluorescence decay curves for aqueous solutions of PUL-OSA,[20,21] and P(MAL/C12),[16] as well as from the steady-state fluorescence quenching experiment for aqueous solutions of CHP.[32] Reproduced with permission from ref 20. Copyright (2020) American Chemical Society.

Fig. 4 SAXS profiles for PUL-OSA samples in 0.05 M aqueous NaCl at 25 °C[20,21] (a) and for C12CMA samples in 0.15 M aqueous NaCl at 25 °C,[19] as well as SANS profiles for CHP and the mother pullulan sample P100 in phosphate buffer at 25 °C.[36] Profiles in Panels a and b other than P100 and C12CMA08-90 are shifted vertically by the factor A indicated in the panel. Solid and dashed curves indicate fitting results explained in the text; dot-dash curves are the fitting results by the wormlike chain perturbed by the excluded volume effect.[34,35]

Fig. 5 (a) Aggregation number m of copolymer chains per micelle,[16,20,21,32] (b) the radius of gyration $\langle S^2 \rangle^{1/2}$,[6,19-22] and (c) the shrinking factors g'_H and g'_S for micelles of amphiphilic random and alternating copolymers.[17,20,21,32]

Fig. 6 *DS* dependences of n_{loop} and $\overline{R}_{core}$ (a), as well as $n_c/(n_c + n_l)$ (b) for PUL-OSA,[20,21] C12CMA,[19] and P(MAL/C12)[17] micelles.

Supporting Information

Dependences of the micellar structure on the degree of substitution and degree of polymerization

Let us consider a single copolymer chain comprising $N_{0,1}$ monomer units with contour length h. The total contour length of the copolymer chain is $hN_{0,1}$. As shown in Figure S1, when the copolymer chain bears hydrophobes at both ends, it forms a loop by association of the two hydrophobes in water. The loop chains associate intermolecularly to form a flower micelle. With increasing DS of the hydrophobic group, the single copolymer chain form multiple loops, and then a micelle. According to the wormlike chain statistics, the loop cannot be formed, if the contour length is shorter than $l_{loop} \equiv 1.6q$, where q is the persistence length of the chain. Thus, when the contour distance between the nearest-neighbor hydrophobic groups h/DS is equal to l_{loop}, the copolymer chain forms minimum-size loops, and when $DS > h/l_{loop}$, all hydrophobes cannot include the hydrophobic core.

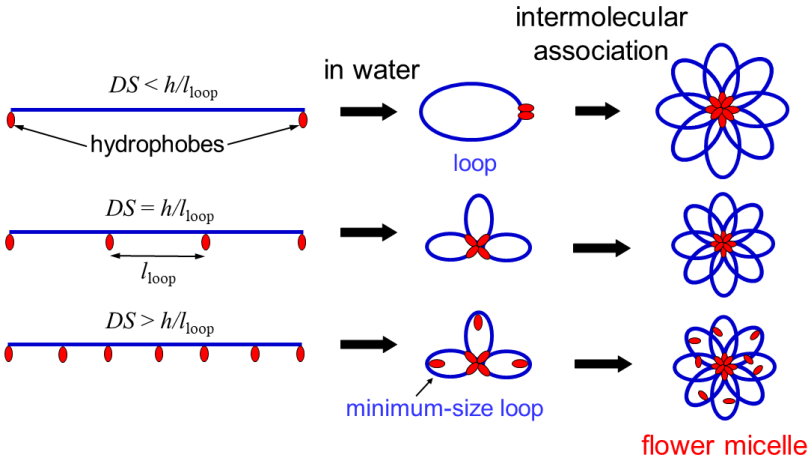

Figure S1. Schematic illustrations of amphiphilic copolymer chains with different DS, forming the micelle in water.

In the last case of Figure S1, the flower micelle formed is assumed to comprise n_{loop} loop chains. Then, we have the relation $l_{loop}n_{loop} = mN_{0,1}h$, where $N_{0,1}$ is the degree of polymerization and m is the aggregation number of the copolymer chain forming the flower micelle. When $N_{0,1} = l_{loop}n_{loop}/h$ ($\equiv N_{0,u}$), $m = 1$, i.e., the flower micelle is formed by a single copolymer chain, which is called as the unimer micelle. When $N_{0,1} > N_{0,u}$, the remaining chain after forming the unit flower micelle can form another unit flower micelle(s). If the contour length of the remaining chain is shorter than $N_{0,u}h$, another unit flower micelle is formed by intermolecular association. The formed multi-core flower micelle is referred to as the flower necklace.

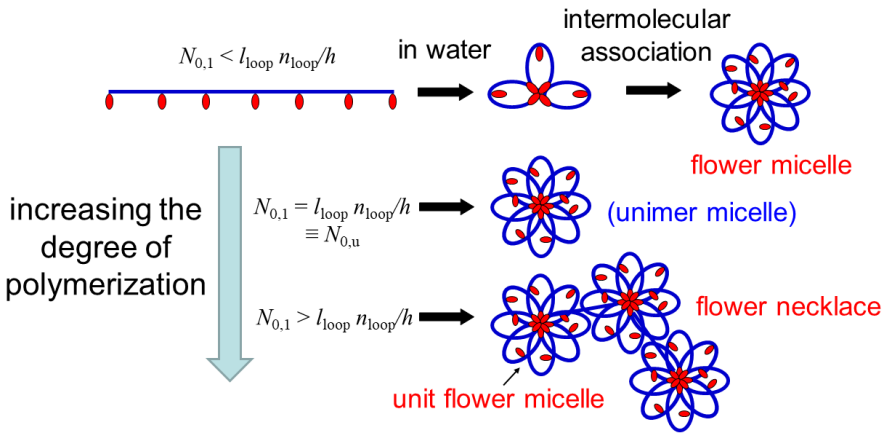

Figure S2. Schematic illustrations of amphiphilic copolymer chains with different degrees of polymerization, forming the micelle in water.

Particle scattering function and shrinking factors for the randomly branched polymer

Let us consider randomly branched polymers consisting of Gaussian subchains. The branched polymers have total n segments and m branch points. The branch points are f functional, and distribute randomly along the polymer chain. The numbers n, m, and f are fixed. The number of segments within a subchain is distributed randomly, although the total number is fixed to be n. The total number of subchains p is given as

$$p = (f-1)m + 1 \tag{S1}$$

Even if n, m, f, and p are fixed, there are many structural isomers for the randomly branched polymer.

The Nth moments of the distribution function for the distance $R_{i_\lambda j_\mu}$ between ith segment of λth subchain and jth segment of μth subchain within the branched polymer chain are given by

$$\langle {R_{i_\lambda j_\mu}}^N \rangle = \begin{cases} A_N \left| j_\mu - i_\lambda \right|^{N/2} & (\lambda = \mu) \\ A_N \left(i_\lambda + n_{\lambda\mu} + j_\mu \right)^{N/2} & (\lambda \neq \mu) \end{cases} \tag{S2}$$

with

$$A_N = \begin{cases} \dfrac{(N+1)!}{(N/2)!}\left(\dfrac{1}{6}a^2\right)^{N/2} & (N = 0 \text{ and positive even integers}) \\ \dfrac{2}{\sqrt{\pi}}\left(\dfrac{1}{2}N+1\right)!\left(\dfrac{2}{3}a^2\right)^{N/2} & (N = -1 \text{ and positive odd integers}) \end{cases} \tag{S3}$$

where a is the segment length, and $n_{\lambda\mu}$ is the total number of segments in the subchains lying between the λth and μth segments. Kurata and Fukatsu[1] calculated the sum of $\langle {R_{i_\lambda j_\mu}}^N \rangle$ over all the possible pairs of i_λ and j_μ for the randomly branched polymer (all possible structural isomers) with fixed n, m, f, and p, by means of generating functions. The result is given by

$$\sum_{(i_\lambda j_\mu)} \langle R_{i_\lambda j_\mu}^{2N'} \rangle = \frac{A_N\,(p-1)!\,n^{N'+2}}{(N'+1)(N'+2)\Gamma(p+N'+2)} \left\{ p\Gamma(N'+3) + (N'+1)(N'+2) \left[\frac{1}{2} f(f-1) m \Gamma(N'+2) + \frac{1}{2}(f-1)^2 m(m-1) \sum_{\nu=1}^{m-1} \frac{\Gamma(\nu+N'+2)(fm-m-\nu)!(m-2)!}{(\nu+1)!(fm-m)!(m-\nu-1)!} (f-1)^{\nu-1} (f\nu-2\nu+f) \right] \right\} \tag{S4}$$

where $N' \equiv N/2$ and $\Gamma(x)$ is the Gamma function of x (eq 24 in the original paper[1] is incorrect).

As shown in Fig. 4c of the text, the SANS profile indicates that CHP forms self-aggregates in aqueous medium. If the self-aggregate is regarded as the randomly branched polymer, the SANS profile can be calculated by

$$\frac{R_{\theta,\mathrm{N}}}{K_\mathrm{n} c} = \frac{M_\mathrm{w} P(k)}{1 + 2A_2 M_\mathrm{w} P(k) c} \tag{S5}$$

with the weight average molar mass M_w and the particle scattering function $P(k)$ given by

$$P(k) = 1 + \sum_{N'=1}^{\infty} \frac{(-1)^{N'} k^{2N'}}{(2N'+1)!} \frac{2}{n^2} \sum_{(i_\lambda j_\mu)} \langle R_{i_\lambda j_\mu}^{2N'} \rangle \tag{S6}$$

Using eq S4, we can also calculate the shrinking factors with respect to the mean square radius of gyration g_S and to the hydrodynamic radius g_H as

$$g_\mathrm{S} \equiv \frac{\langle S^2 \rangle_{\text{random branch}}}{\langle S^2 \rangle_{\text{linear}}} = \frac{6}{p(p+1)(p+2)} \left[p^2 + \frac{1}{2}(f-1)^2 m(m-1) \sum_{\nu=1}^{m-1} \nu \frac{(fm-m-\nu)!(m-2)!}{(fm-m)!(m-\nu-1)!} (f-1)^{\nu-1} (f\nu-2\nu+f) \right] \tag{S7}$$

$$g_\mathrm{H} \equiv \frac{R_{\mathrm{H,random\ branch}}}{R_{\mathrm{H,linear}}} = \frac{3\sqrt{\pi}\Gamma(p)}{4\Gamma(p+\frac{3}{2})} \left[p + \frac{1}{4} f(f-1) m + \frac{1}{2}(f-1)^2 m(m-1) \sum_{\nu=1}^{m-1} \frac{(2\nu+2)!}{[2^{\nu+1}(\nu+1)!]^2} \frac{(fm-m-\nu)!(m-2)!}{(fm-m)!(m-\nu-1)!} (f-1)^{\nu-1} (f\nu-2\nu+f) \right] \tag{S8}$$

1. Kurata M, Fukatsu M. Unperturbed dimension and translational friction constant of branched polymers. J Chem Phys. 1964; 41: 2934-2944.